Title	Formation of stacking-fault tetrahedra in aluminum irradiated with high-energy particles at low-temperatures
Author(s)	Satoh, Y; Yoshiie, T; Mori, H; Kiritani, M
Citation	PHYSICAL REVIEW B (2004), 69(9)
Issue Date	2004-03
URL	http://hdl.handle.net/2433/39863
Right	Copyright 2004 American Physical Society
Type	Journal Article
Textversion	none; publisher

Formation of stacking-fault tetrahedra in aluminum irradiated with high-energy particles at low-temperatures

Y. Satoh,[1,*] T. Yoshiie,[1] H. Mori,[2] and M. Kiritani[3,†]

[1]*Research Reactor Institute, Kyoto University, Kumatori-cho, Sennan-gun, Osaka, 590-0494 Japan*
[2]*Research Center for Ultra-High Voltage Electron Microscopy, Osaka University, 2-1, Yamadaoka, Suita, Osaka, 565-0871 Japan*
[3]*Academic Frontier Research Center for Ultra-high-speed Plastic Deformation, Hiroshima Institute of Technology,*
2-1-1, Miyake, Saeki-ku, Hiroshima, 731-5193 Japan

Stacking-fault tetrahedra (SFT) are typical vacancy clusters in fcc metals. SFT have been, however, considered to be unstable in aluminum because of its high stacking-fault energy, until the recent finding of SFT in thin aluminum foils subjected to a tensile fracture. This study confirmed that SFT form in aluminum following irradiation with high-energy particles. In electron irradiation, SFT with an average size of 2 nm formed below 203 K, while a larger irradiation intensity at lower temperature induced SFT with a larger number density. Irradiation with 60-keV Al^+ ions induced SFT below room temperature, although the defect yield (the ratio of the number of defect clusters to the number of incident ions) was about 10^{-3}, considerably smaller than that in the other fcc pure metals. With neutron irradiation below 15 K to a fluence of 2×10^{21} neutrons m^{-2}, SFT were not observed at room temperature. Instead, dislocation loops were observed to form and to disappear during observation with 120-kV electrons that do not cause atomic displacements. Tensile fracture of aluminum thin foil induced SFT at up to 400 K, which is close to the temperature at which SFT become unstable in isochronal annealing experiments. These results suggest that a high concentration of vacancies at lower temperature tends to cause SFT to form rather than vacancy-type dislocation loops in aluminum.

I. INTRODUCTION

The first observation of point-defect clusters with transmission electron microscopy (TEM) was made by Hirsch *et al.* in 1958, for vacancy-type dislocation loops in aluminum induced by quenching from high temperatures.[1] Since then, several types of point-defect clusters have been found in various metals subjected to quenching, mechanical deformation, and irradiation with high-energy particles. These studies have contributed to our understanding of the nature and processes of point defects and their clusters. While clusters of self-interstitial atoms always appear as dislocation loops, vacancy-type defect clusters show variation in fcc metals: perfect- and faulted-dislocation loops, stacking fault tetrahedra (SFT), and voids. As was reviewed by Eyre[2] and Zinkle, Seitzman, and Wolfer,[3] all types of vacancy clusters have been reported to form in each fcc metal on employing the above methods under appropriate conditions. But aluminum was an exception: the formation of SFT was not reported. The absence of SFT was interpreted from the higher stacking-fault energy in aluminum than in the other fcc metals. A calculation of the static formation energy of vacancy clusters based on an elastic continuum expression supported the interpretation that the SFT structure is less stable in aluminum.[3]

Recently, in a study of the tensile fracture of metal foils, SFT were found to form in aluminum as well as in other fcc metals.[4] In the tip portion of fractured fcc metals, dislocations were almost absent while a large number of SFT and vacancy-type dislocation loops were observed. The typical concentration of vacancies retained in vacancy clusters exceeded 10^{-3}. It was proposed that a new mechanism of plastic deformation without dislocation is activated in the fracture of metal foils.[4,5]

The present paper reexamines whether or not irradiation with high-energy particles causes SFT to form in aluminum. We irradiated aluminum with high-energy electrons, ions, and neutrons under several conditions and surveyed vacancy clusters in detail, employing an improved technique for observing small SFT with TEM.[6] We confirmed that SFT form in aluminum following intense irradiation with high-energy electrons and ions at low temperatures. To examine the efficiency of the formation, we examined the temperature range of the SFT formation induced by tensile fracture. We also performed annealing experiments on SFT in aluminum. Finally, we discuss the optimal conditions for the formation of SFT in aluminum.

II. EXPERIMENTAL PROCEDURE

An aluminum block of 99.999% purity was rolled into foils 0.1 mm thick and annealed at 873 K for 1 h. Thin-foil specimens for TEM were prepared by electropolishing in a $HClO_4 : CH_3OH$ (1:4) solution and then irradiated with high-energy particles.

The electron irradiation was generated with a high-voltage electron microscope (H-3000) at Osaka University, operating at an accelerating voltage of 2 MV. The irradiation temperature ranged from 113 to 253 K in steps of about 50 K, using a low-temperature stage with liquid nitrogen. The maximum electron current density was 2.5×10^{24} electrons $m^{-2} s^{-1}$, which corresponds to a damage rate of 1.4×10^{-2} dpa s^{-1} according to the collision cross section calculated by Oen[7] and applying 15 eV for the threshold energy of atomic displacement.[8] The magnitude of damage formation is expressed by the number of times each atom is displaced from its lattice site, i.e., displacements per atom (dpa).
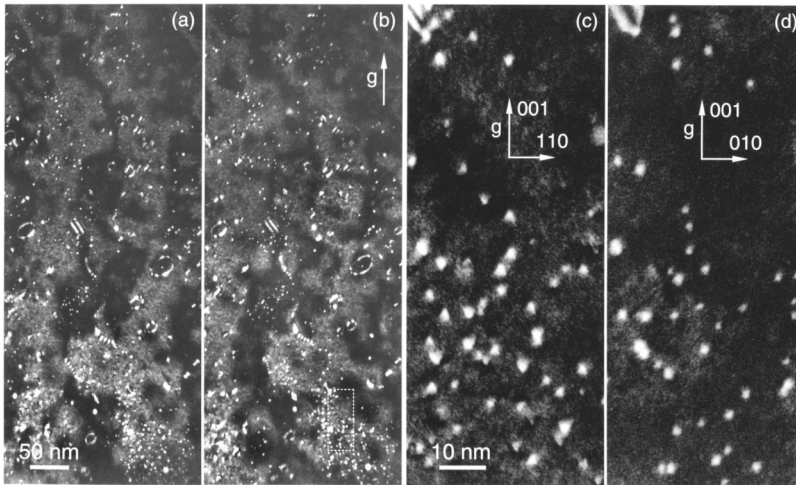
FIG. 1. (a), (b) Stereo-pair micrograph of aluminum irradiated with 2-MV electrons, 1.5×10^{24} electrons $m^{-2} s^{-1}$ for 1200 s at 113 K. Micrographs (c) and (d) correspond to the area bounded with dashed lines in (b). They were taken at a larger magnification in both directions close to $\langle 110 \rangle$ and $\langle 100 \rangle$, respectively.

Self-ion irradiation was generated with a heavy-ion accelerator attached to a sputter ion gun at the Research Reactor Institute of Kyoto University. The accelerating voltage was 60 kV, and the ion current density was 3×10^{16} ions $m^{-2} s^{-1}$. The irradiation temperature ranged from 123 K to room temperature in about 50-K steps. According to a calculation with the TRIM-3D code, the average depth of incident ions is 86 nm and the maximum damage rate is 5.7×10^{-3} dpa s^{-1} around the ion range.

Neutron irradiation was generated with the Low Temperature Loop (LTL) facility at the Kyoto University Reactor (KUR). The irradiation temperature was lower than 15 K, and the fluence of fast neutrons (>0.1 MeV) was 2.7×10^{21} neutrons m^{-2} following irradiation for 75 h. The number of point defects produced was considerably smaller than in the above two cases: the total atomic displacement was 6.2×10^{-4} dpa, and the damage rate was as low as 2.3×10^{-9} dpa s^{-1}. However, neutron irradiation induces cascades of larger primary recoil energy, which results in the production of a large number of point defects in spatially localized regions. For example, 38% and 9% of all point defects produced are formed from primary knock-on atoms (PKA's) whose recoil energy is larger than 100 and 300 keV, respectively.

After the irradiation with electrons or ions, the temperature of the specimen was raised to room temperature within a few hours. By contrast, we waited at least 3 weeks before handling the specimens irradiated with neutrons. During this period, the specimens were kept in liquid nitrogen and the specimen temperature was raised to room temperature a few hours before TEM observation. The microstructure was observed with an electron microscope, JEOL 2010, operating at 120 kV so as to avoid atomic displacement. In order to resolve small defect clusters, we mainly utilized weak-beam dark-field images ($\mathbf{g}=002$). The parameter $s(002)$ that denotes deviation from the exact Bragg condition was $(1.2–2.0) \times 10^{-1}$ nm^{-1} in most observations.

In order to compare the temperature dependence of SFT formation, we also examined the tensile fracture at several temperatures. The specimen was 30 μm thick, 5 mm wide, and 15 mm long and had a notch at the midpoint for initiating fracture. Then it was annealed under the same conditions

as for irradiation. The respective ends of the specimen were held with two tweezers, and the specimen was torn apart by tension. The atmosphere and temperature of the fracture were as follows: liquid nitrogen (80 K), methanol (190 K), air (300 K), or glycerol (350 and 400 K). A few seconds after the tensile fracture, the specimen was dipped in methanol at room temperature and was observed with TEM. The tip portion of the fractured specimen has thickness suitable for direct observation with TEM (<100 nm).[4] We observed the specimen without applying a thinning procedure. The time elapsed between the tensile fracture and the TEM observation was within a few hours in most cases.

III. EXPERIMENTAL RESULTS

A. Electron irradiation

Figures 1(a) and 1(b) are a stereo pair micrograph of the area that was irradiated with 2-MV electrons for 1200 s. The irradiation temperature was 113 K, about the lowest temperature achieved using the liquid nitrogen stage attached to the high-voltage electron microscope (HVEM). In addition to well-grown interstitial-type dislocation loops, a large number of small defect clusters are observed almost homogeneously in the specimen foil. The area bounded by the dashed line in Fig. 1(b) was observed at a larger magnification along the $[1\bar{1}0]$ direction [Fig. 1(c)] and [100] direction [Fig. 1(d)]. The images of the small defect clusters have, respectively, triangular and square shapes, which confirms that the defects are SFT. The average size of the SFT is about 2 nm and corresponds to aggregates of a few tens of vacancies.

At the lowest irradiation temperature 113 K, the defect structure variation with the irradiation time was compared among three irradiation intensities. The upper row in Fig. 2 shows irradiation at the highest beam intensity which corresponds to a point-defect production rate of 1.4×10^{-2} dpa s^{-1}. SFT can already be observed after irradiation for 10 s, and the size and number density of SFT do not increase much after 30 s. The number density was about 2×10^{23} m^{-3} at saturation. On the other hand, interstitial-type dislocation loops ($\mathbf{b}=a/3[111]$) nucleate in the initial stage of irradiation and continue to grow with the irradiation
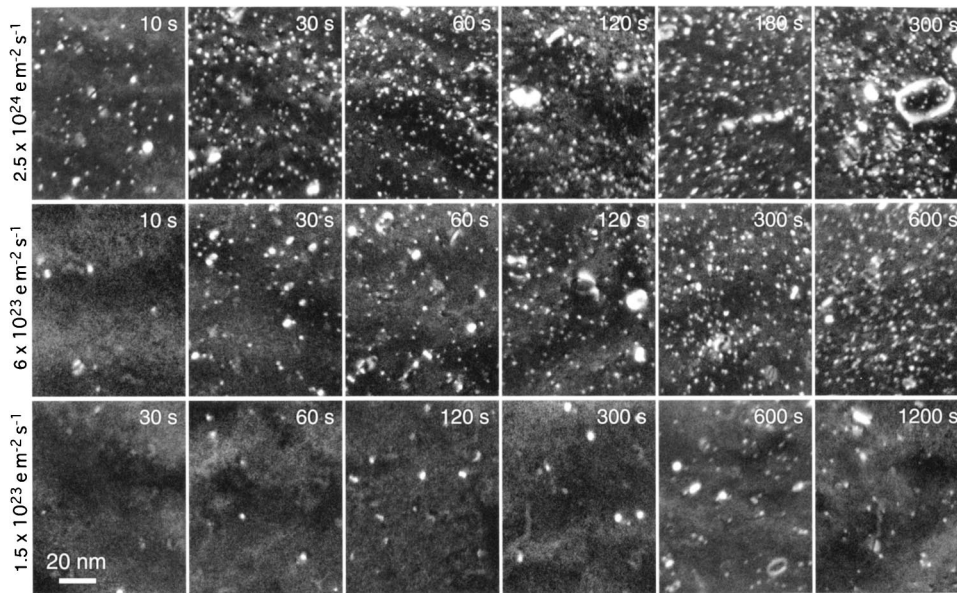
FIG. 2. Variation of defect structure in 2-MV electron-irradiated aluminum with the irradiation time and irradiation intensity. Top, middle, and bottom rows correspond to damage rates for 1.4×10^{-2}, 3.5×10^{-3}, and 9×10^{-4} dpa s^{-1}, respectively. The irradiation temperature was fixed at 113 K.

time. In the middle row of the figure where the irradiation intensity is a quarter that of the upper row, the number density of SFT builds up slower. As compared with the highest irradiation intensity, the number density of SFT at saturation decreases by 20%–30%, but there is no significant difference in the size of SFT. In the bottom row of the figure, the intensity is lowered another quarter. The production rate of point defects is about 10^{-3} dpa s^{-1}, approximately equal to that of the HVEM of the first generation. Even at this intensity, SFT formed after a considerable incubation period. Their number density is an order of magnitude smaller than that at the highest intensity.

Figure 3 shows defect structures induced by 300 s irradiation at 113, 153, 203, and 253 K, to examine the irradiation temperature dependence of SFT formation. SFT formed following irradiation at 153 K, although their number density decreased to almost half that at 113 K. Very few SFT were observed in the area irradiated at 203 K, which is around the critical temperature. No SFT were observed after irradiation at 253 K. Again, the SFT size depended little on the irradia-

tion temperature. However, interstitial-type dislocation loops were observed at all the temperatures examined and grew faster at higher irradiation temperatures.

We note that small dislocation loops in addition to well-grown interstitial-type dislocation loops were observed at relatively high irradiation temperatures where the formation of SFT becomes difficult. Because the conventional inside-outside contrast method did not determine the nature of these small dislocation loops, we applied an identification method which utilizes electron irradiation.[9–11] With this method, small dislocation loops are irradiated with a weak electron beam at a temperature where vacancies are thermally mobile. After the start of irradiation, the point-defect concentration quickly reaches a steady state, where the migration efficiency (a product of the concentration and mobility of point defects) is balanced between interstitial atoms and vacancies. In this steady state, interstitial-type dislocation loops grow and vacancy-type dislocation loops shrink because edge dislocations prefer to absorb more interstitials than vacancies due to the bias effect of dislocations.
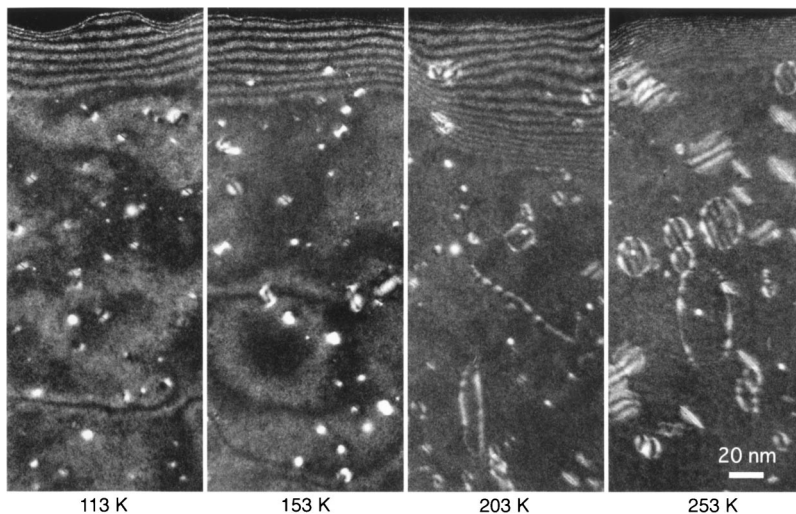

FIG. 3. Irradiation temperature dependence of the defect structure in aluminum. Irradiation for 300 s with a damage rate of 8.5×10^{-3} dpa s^{-1}.
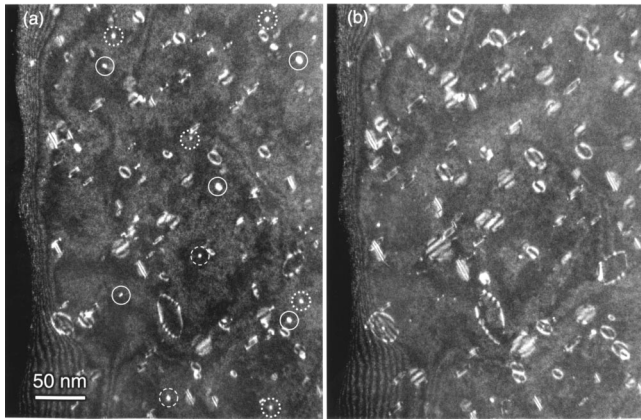
FIG. 4. (a) Defect structure in aluminum irradiated with 2-MV electrons for 120 s at 253 K. (b) The area shown in (a) was irradiated with 200-kV electrons for 900 s at 300 K. The small dislocation loops that were grown, unchanged, and disappeared during 200 kV irradiation are shown with solid, dashed, and dotted circles, respectively in (a).

Figure 4(a) shows a typical defect structure containing small dislocation loops, which was induced by irradiation with 2-MV electrons for 120 s at 253 K. The small dislocation loops of interest are shown with circles. Figure 4(b) shows the identical area after irradiation with 200-kV electrons for 900 s at room temperature. Large dislocation loops, which are of interstitial type, increase in size at 200 kV irradiation with a few exceptions that is thought to escape to the specimen surfaces by gliding motion after unfaulting. In contrast, the behavior of the small loops varied. Among 16 loops examined, 7 loops grew, 6 shrank or disappeared, and 3 did not show apparent changes.

B. Self-ion irradiation

Figure 5 shows the small point-defect clusters induced by irradiation with 60-keV Al$^+$ ions at 120 K, which are observed along two typical directions [$1\bar{1}0$] and [100]. The figure confirms that self-ion irradiation forms SFT in aluminum. Figure 6 compares defect-cluster formation among several irradiation temperatures at the constant irradiation dose of 3.6×10^{18} ions m^{-2}. The top and bottom rows of the figure show, respectively, defect structures in the area thinner and thicker than the range of incident ions. In the thinner area, only SFT are formed, while both SFT and interstitial-type dislocation loops are formed in the thicker area. The number of SFT decreases as the irradiation temperature increases, similar to the electron irradiation. Because a few SFT are still observed after the ion irradiation at room temperature, the temperature range of SFT formation extends to higher temperatures on irradiation with ions than electrons.

Figure 7 shows the defect structure variation with ion dose at a constant irradiation temperature 120 K. As the ion dose increases, the number of observed SFT increases both in the thinner area (top row of the figure) and thicker area (middle row), while the SFT size is almost unchanged. Interstitial-type dislocation loops in the thicker area increase in number density and size with increasing ion dose. Of note
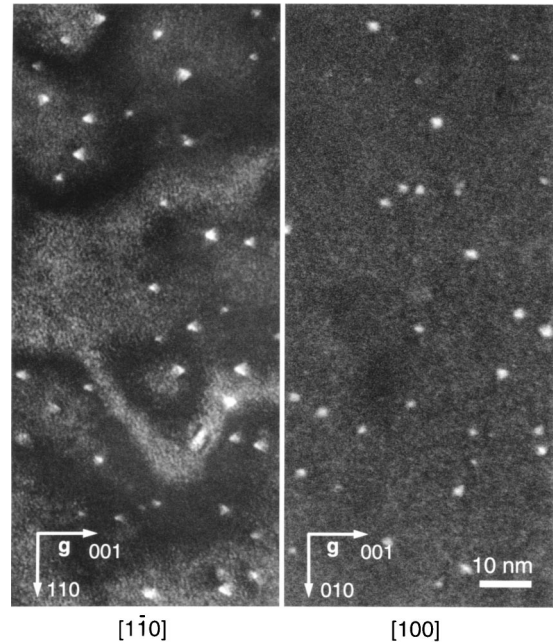

FIG. 5. Small point-defect clusters induced by the irradiation with 60-keV Al$^+$ ions, at 120 K. The two figures show typical images of small defect clusters observed along directions close to $\langle 110 \rangle$ and $\langle 100 \rangle$, respectively.

is that the number of SFT formed in aluminum is much less than in the other pure fcc metals. This is clearly seen in the bottom row of the figure, which shows the defect structure induced in copper that was irradiated simultaneously with aluminum specimens shown in the top and middle rows.

Table I shows the incident ion dose, the areal number density of SFT, and a parameter "defect yield" that is the ratio of the number of SFT to the number of incident ions. The defect yield in aluminum is of the order of 10^{-3}. The small defect yield at small dose contains considerable ambiguities because the number density of SFT is quite small. In contrast, the defect yield for copper is about 0.1 by Al ion irradiation. The self-ion irradiation of copper is expected to result in a larger defect yield. For example, the defect yield is about 0.5 in 30-keV self-ion irradiated copper.[12] The defect yield in copper drops to 0.012 at a large dose, the reason for which is clearly seen in Fig. 7: a saturation in the number density of SFT due to spatial overlapping of cascade events.

C. Neutron irradiation

We performed two experimental runs of neutron irradiation and post-irradiation observation. The irradiation conditions, such as total neutron fluence, neutron flux, and irradiation temperature, are equal to each other. The difference is in the period that the specimen was kept in liquid nitrogen after irradiation below 15 K until the TEM observation at room temperature: one was 23 days and the other was 14 months. In both specimens, small defect clusters were observed with a small number density. The majority of the defect clusters have a contrast of dislocation loops, and the formation of SFT was not identified. There were minor dif-
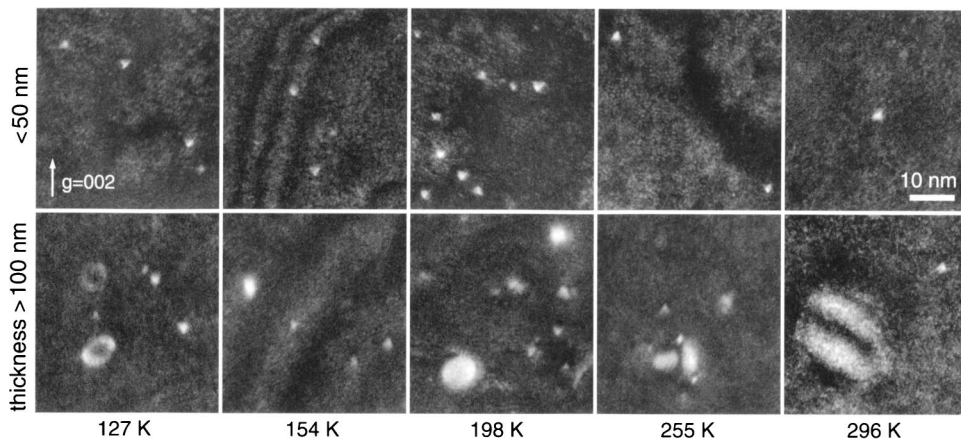
FIG. 6. Temperature dependence of SFT formation at the constant irradiation dose of 3.6×10^{18} ions m^{-2}. The top and bottom rows correspond to the area whose specimen thickness is about 50 and 100 nm, respectively.

ferences in the behavior of the defect clusters between the two specimens as is described below in detail.

In the specimen observed 23 days after the irradiation, defect clusters were observed with a number density of about 2×10^{20} m^{-3}. During observation at 120 kV, some defect clusters newly appeared as shown in the top row of Fig. 8, although atomic displacements were not expected to occur at this accelerating voltage. They are not contaminations: a stereo observation confirmed that the defect clusters are inside the specimen foil. Careful observation revealed that defect clusters did not simply appear, but some disappeared under illumination, although their total number density increases with illumination time: about 1×10^{21} m^{-3} after illumination for 6 h. Also, the behavior of individual defect clusters is not simple: some defect clusters shrink after growing for a certain period and others vice versa. Because the number density of defect clusters was not increased in the area without illumination, illumination rather than aging at room temperature is thought to be responsible for the behavior of defect clusters. On the other hand, another illumination that started a week after heating the specimen to room temperature did not induce significant changes in defect clusters.

In the specimen that was observed 14 months after the neutron irradiation, the initial number density of defect clus-

ters was about 1×10^{20} m^{-3}. As shown in the bottom row of Fig. 8, again, some defect clusters disappear and others newly appear under observation at 120 kV. The total number of defect clusters, however, decreased by half after illumination for 6 h. Larger defect clusters seem to be dislocation loops, and no formation of SFT was identified.

Figure 9 shows the variation in defect clusters in the latter specimen during electron irradiation at 200 kV. Again, the behavior of the defect clusters is not simple: all types—namely, grown, shrunk, and unchanged defect clusters—were observed. We note that weak electron irradiation induced new defect clusters at a later stage.

D. Tensile fracture

SFT in aluminum were first observed in thin-foil specimens subjected to tensile fracture at room temperature.[4] In this section we do not go into detail as to the mechanism of the tensile fracture, but it is useful to examine the efficiency of tensile fracture as a method to induce vacancy clusters to interpret the SFT formation by high-energy particle irradiation described above. Figure 10 shows the temperature dependence of the SFT formation by tensile fracture. The tensile fracture induces SFT up to higher temperatures than
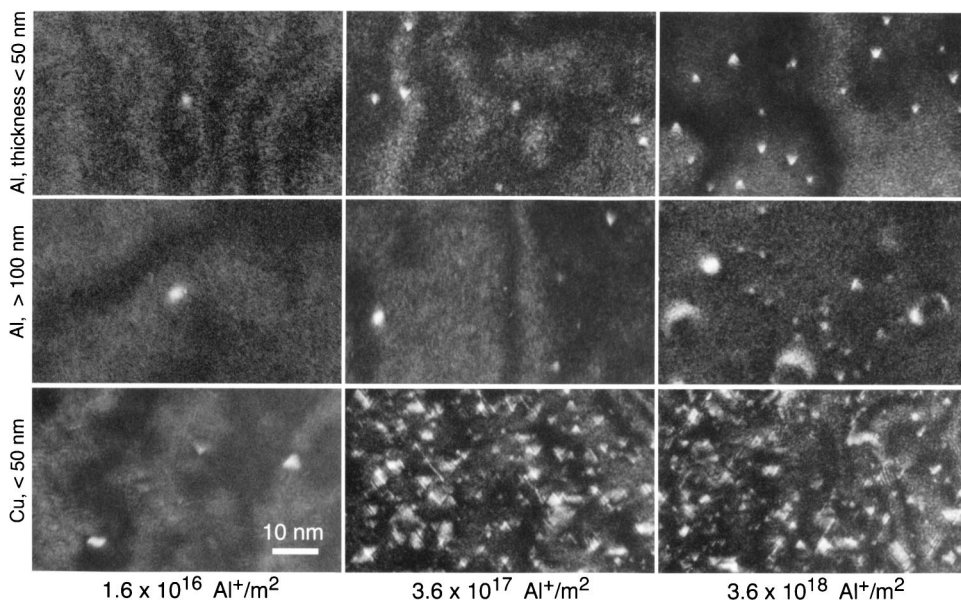

FIG. 7. Variation of defect structure in 60-keV-Al$^+$-ion-irradiated aluminum 50 nm thick (top), 100 nm thick (middle), and copper 50 nm thick (bottom) with the incident ion dose. The irradiation temperature was fixed at 120 K.

TABLE I. Areal number density of SFT and defect yield in aluminum and copper irradiated with Al^+ 60-keV ions at 120 K.

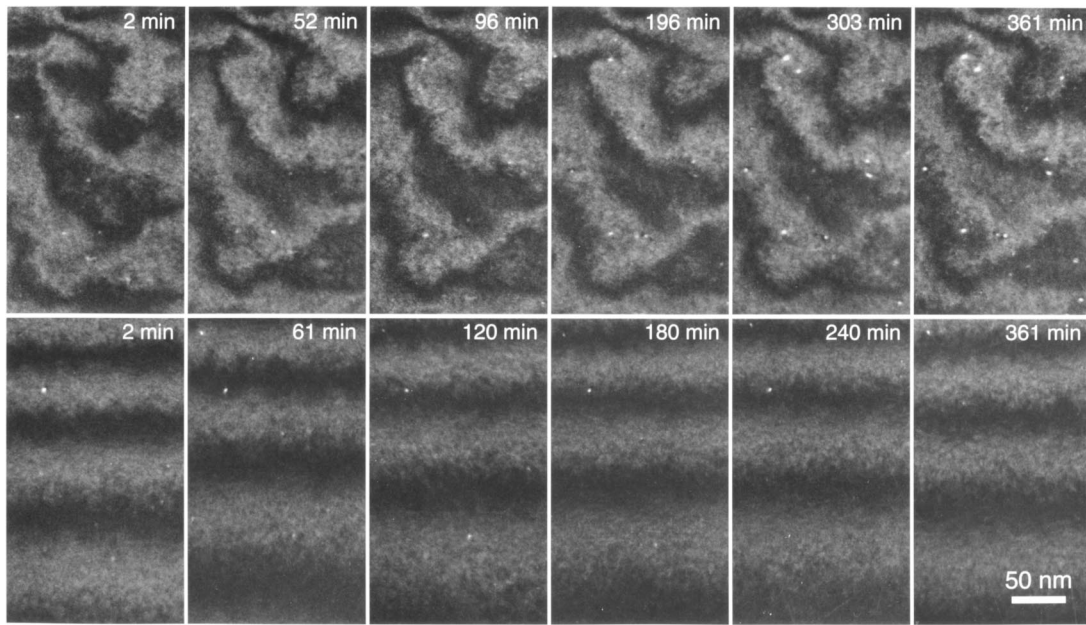| Ion dose (m^{-2})	Al		Cu	
	Areal number density of SFT (m^{-2})	Defect yield	Areal number density of SFT (m^{-2})	Defect yield
1.6×10^{16}	$< 4 \times 10^{12}$	<0.0003	1.2×10^{15}	0.08
3.6×10^{17}	8×10^{14}	0.002	4×10^{16}	0.12
3.6×10^{18}	7×10^{15}	0.002	4×10^{16}	0.012

FIG. 8. Defect structure in aluminum irradiated with fission neutrons below 15 K and its variation during observation with 120-kV electrons. The fluence of fast neutrons (>0.1 MeV) was 2.7×10^{21} netruons m^{-2} following irradiation for 75 h. After irradiation, the specimens were stored in liquid nitrogen for 23 days (top row) or 14 months (bottom row). The temperature of the specimen was raised to room temperature and the specimen was then observed with TEM.
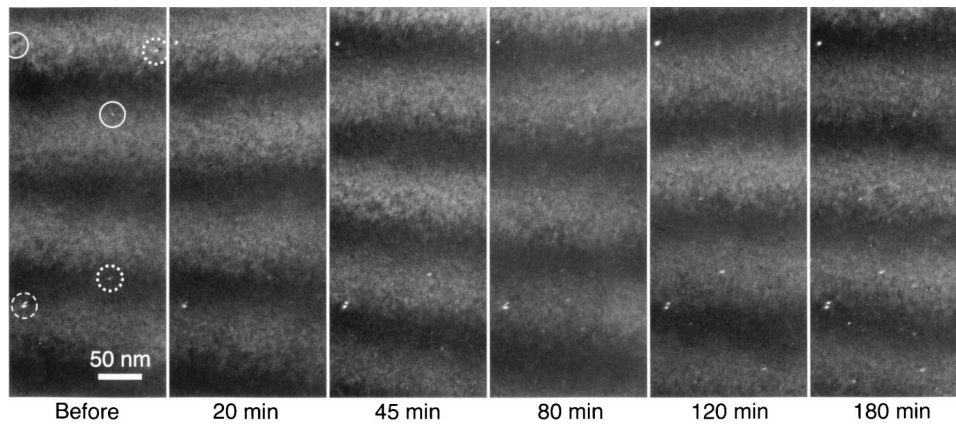

FIG. 9. Defect structure variation in aluminum during the irradiation with 200-keV electrons. The original defect structure was induced by fission neutron irradiation below 15 K followed by storage in liquid nitrogen for 14 months. Defect clusters that were grown, unchanged, and disappeared during 200 keV irradiation are shown with solid, dashed, and dotted circles, respectively.
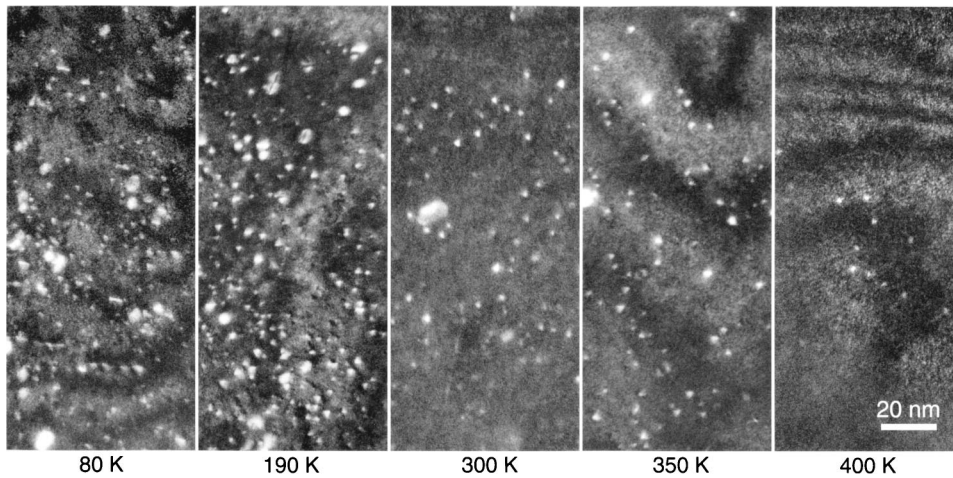
FIG. 10. Defect structure observed in the tip portion of aluminum foil fractured by tension. The atmosphere and temperature of the fracture were liquid nitrogen (80 K), methanol (190 K), air (300 K), and glycerol (350 and 400 K). After the tensile fracture, specimens were dipped into methanol at room temperature within a few seconds.

electron irradiation (Fig. 3) and self-ion irradiation (Fig. 6). In addition to SFT, dislocation loops are observed with a small number density. The nature of large dislocation loops was identified as vacancy type using the inside-outside method, and that of smaller ones was examined by irradiation with 200-kV electrons. Figure 11 shows that SFT disappear first, and simultaneously all the dislocation loops shrink to disappear under electron irradiation, clearly indicating that all defect clusters formed by tensile fracture are of vacancy type.

Finally, we performed an annealing experiment to examine the thermal stability of SFT in aluminum. The SFT were induced by tensile fracture at room temperature, and Fig. 12 shows the result of isochronal annealing for 300 s at each temperature step. The shrinkage and disappearance of SFT starts just above room temperature. Some SFT are observed to grow temporarily, which is thought to be a coalescence of defect clusters or an absorption of vacancies released from smaller clusters that are less stable. Although contamination of the specimen becomes severe at 383 K, almost all SFT had disappeared at this temperature.

As the result of isochronal annealing compared with Fig. 10, the tensile fracture induces SFT a little above the temperature where all SFT are annealed out. We must note that the specimen fractured at high temperatures (Fig. 10) virtually does not involve the annealing effect because it was quickly dipped into methanol at room temperature. It is interesting that SFT are formed by tensile fracture even at the temperature where SFT are annealed out by the subsequent aging.

IV. DISCUSSION

A. Electron irradiation

It has been well established that electron irradiation of metals induces nucleation and steady growth of interstitial-
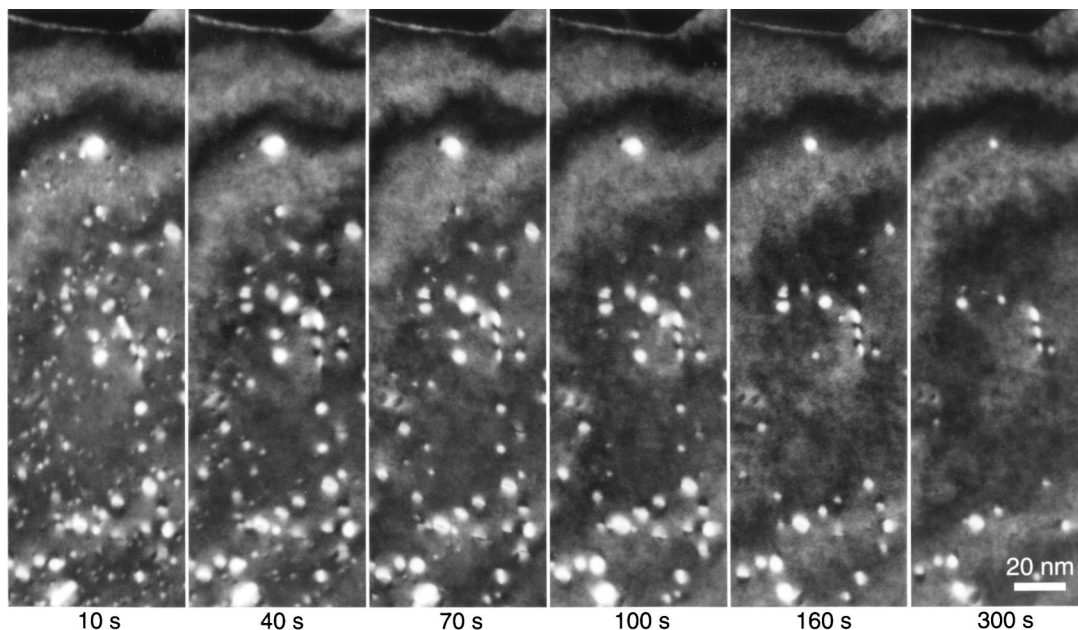

FIG. 11. Defect structure in aluminum induced by tensile fracture at room temperature, and its variation with the time of irradiation with 200-keV electrons at room temperature.
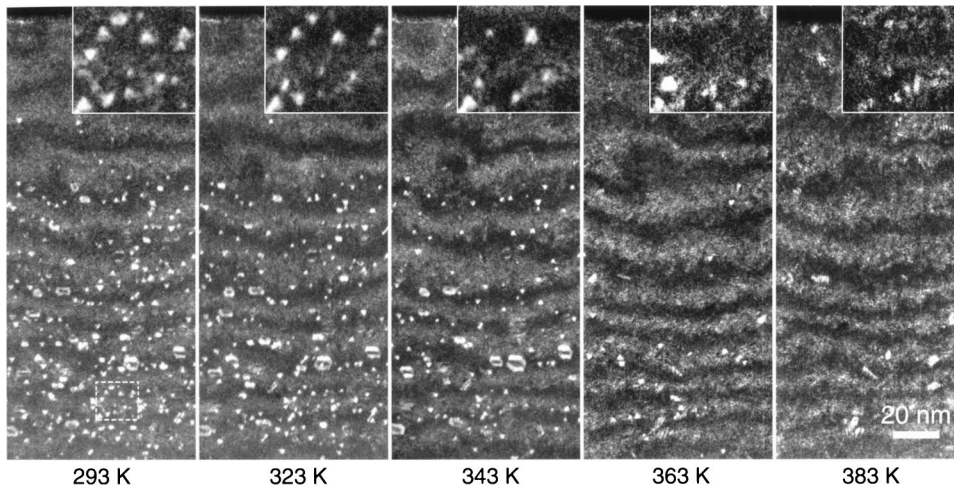
FIG. 12. Defect structure variation during isochronal annealing for 300 s at the respective temperature steps. The original defect clusters were induced by tensile fracture at room temperature. The inset shows the area bounded by dashed lines at a large magnification.

type dislocation loops. It is also known that SFT are formed in fcc metals following irradiation at relatively low temperatures. When the thermal migration of vacancies is not very extensive, the vacancy concentration increases with irradiation time until SFT form.[13] In copper, for example, small SFT (around 2 nm in diameter) are observed uniformly in the specimen foil at a temperature lower than 423 K. The activation energy for vacancy migration in aluminum is 0.65 eV and is smaller than that in copper, 0.72 eV (Ref. 14), and their effective values under electron irradiation are, respectively, 0.55 and 0.60 eV, by a contribution of divacancies.[15] Accordingly, the formation of SFT in a lower-temperature range in aluminum than in copper is reasonable. In addition, the temperature dependence and irradiation intensity dependence of the number density of SFT in aluminum presented above are qualitatively similar to those reported for copper.[16] Therefore, the behavior of SFT in electron-irradiated aluminum is regarded to be the same as that in the other fcc metals.

SFT in pure copper are not stable under electron irradiation, and they repeat formation and disappearance randomly, reflecting the fluctuation of point-defect absorption.[16–18] Although we did not perform an *in situ* observation of SFT in aluminum, the formation and disappearance of SFT is expected because the point-defect absorption is essentially stochastic and also because the SFT are small enough in aluminum.

Next, we discuss briefly the small dislocation loops that were formed following electron irradiation at higher temperatures and are suggested to consist of both interstitial- and vacancy-type dislocation loops. Well-grown interstitial-type dislocation loops nucleate during the peak of interstitial concentration realized at the start of irradiation, while small interstitial-type dislocation loops are thought to nucleate in the later stage of irradiation. We note that, however, the nucleation of loops in the later stage is not observed in copper.[19] On the other hand, as far as the authors know, there is no reliable report that vacancy-type dislocation loops are formed in pure fcc metals by electron irradiation. The possibility of the formation of vacancy-type dislocation loops, however, cannot be excluded because we have frequently observed vacancy-type dislocation loops in aluminum after

quenching and tensile fracture. The nature of these small dislocation loops requires further examination.

B. Ion and neutron irradiation

In pure fcc metals, it has been known that SFT are directly formed from high concentrations of vacancies in a cascade damage region irradiated at relatively lower temperatures. In 14-MeV-neutron-irradiated copper, a single SFT corresponds to a subcascade energy of about 10 keV at room temperature, while smaller subcascades fail to form SFT at elevated temperatures.[20] However, such a direct formation of SFT is not observed in neutron-irradiated aluminum. Then effects of cascade damage were demonstrated by the change of interstitial-type dislocation loops that had been induced by electron irradiation prior to the neutron irradiation.[21]

In the present fission neutron irradiation below 15 K, we did not observe the direct formation of SFT in aluminum, but the presence of small dislocation loops and submicroscopic defects that are invisible with TEM. Some submicroscopic defects are thought to rearrange and/or combine to form visible defect clusters following subthreshold electron illumination, probably due to a mechanism similar to the radiation-induced migration of point defects.[22] Simultaneously, the other invisible defects disappeared with time at room temperature or following subthreshold electron illumination.

Also heavy-ion irradiation induces SFT in various fcc metals.[12,23–25] The areal number density of SFT increases with increasing ion dose until spatial overlapping of cascades occurs, suggesting that vacancy clusters are produced from cascade collisions. But the formation of SFT was not reported previously for ion-irradiated aluminum.

We must note that SFT were not formed by fission neutron irradiation, but by ion irradiation, although neutron irradiation produces PKA's with a larger recoil energy than the incident energy of the self-ion irradiation. We also note that the production rate of point defects was much larger in ion irradiation (5.7×10^{-3} dpa s^{-1}) than in fission neutron irradiation (2.3×10^{-9} dpa s^{-1}). These results suggest that a single cascade event does not form SFT in aluminum even though the primary recoil energy exceeds several hundred keV.

A simple interpretation is as follows: cascade collisions do not have any apparent effect on SFT formation because the vacancies produced by cascades are more dilute in aluminum than in copper or gold.[26] Then free vacancies that have escaped from the cascade damage zone aggregate to form SFT in a similar manner as in the electron irradiation presented in Sec. III A. But this interpretation may be oversimplified: the effect of localized vacancies produced by cascade collisions cannot seem to be ignored for SFT formation in aluminum because ion irradiation forms SFT up to higher temperatures than electron irradiation even though the production rate of point defects is smaller in ion irradiation.

Then another interpretation is that a single cascade induces submicroscopic defects that develop into SFT by some additional point-defect processes during the continuous irradiation at a large damage rate. Although the number density of SFT at only three ion doses was examined in the above experiment, the extremely small defect yield at small dose will correspond to an accumulation phase of invisible defects. The formation of invisible defects was suggested in Cu, Ni, and Au irradiated with 14-MeV neutrons at room temperature.[27] The invisible defect changes into visible defects (SFT) with the impact effect of a cascade produced in the vicinity of the invisible defect. The number density of visible defect clusters builds up in proportion to the square of the irradiation dose in the smaller dose range and then increases linearly with ion dose in the larger dose range, which is explained from a kinetic analysis of a simple model of the impact effect of cascades.[27] In the self-ion irradiation of aluminum, however, further investigation is necessary to determine the point-defect process to change the invisible defect cluster into SFT.

C. Tensile fracture

In the tensile fracture of metal foils, SFT are formed up to the temperature where the thermal stability of SFT becomes serious. This suggests that vacancies of extremely high density are produced by tensile fracture, although the mechanism of the deformation is out of the scope of this paper. Next, we note the shrinkage of SFT in the isochronal annealing. Because there has been no experimental evidence of the formation of self-interstitial atoms and their clusters in tensile fractures, the shrinkage is thought to be caused by the emission of vacancies from SFT. Some SFT in Fig. 12 seem to shrink while keeping their triangular shape, suggesting that SFT shrink without converting to dislocation loops.

D. Process of SFT formation in aluminum

We consider a growth process of vacancy-type defect clusters in aluminum, especially how SFT form under intense irradiation at low temperatures. Figure 13 shows the formation energy of three defect configurations in copper and aluminum calculated by Zinkle *et al.*[3] The figure also shows, in the same scale, the size distributions of vacancy clusters observed in typical experiments. We note that the number of vacancies in the defect cluster was simply converted from the area of the defect image that was measured on a linear
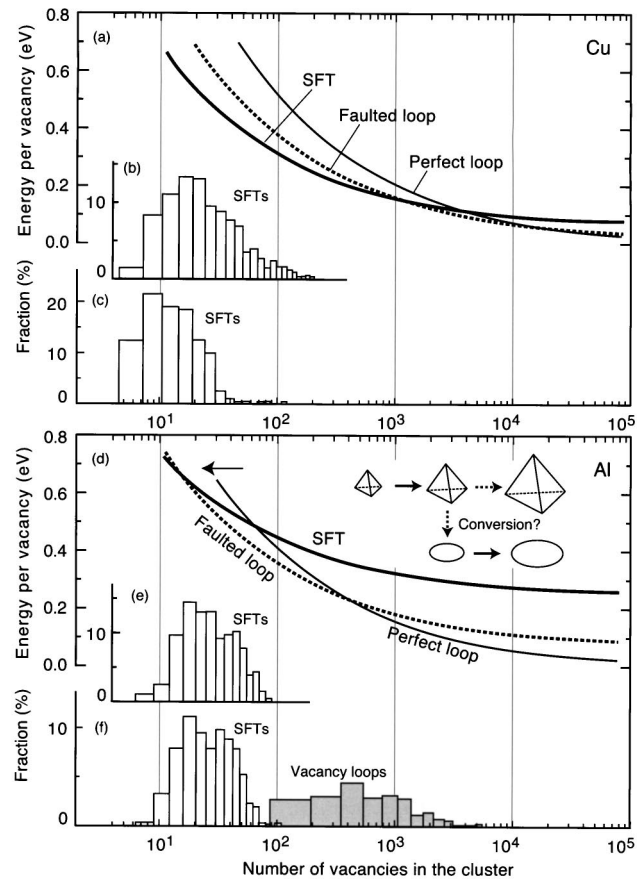

FIG. 13. Variation of formation energy (expressed as the energy per vacancy) of vacancy-type defect clusters in copper (a) and aluminum (d), as a function of defect size (the number of vacancies in the defect cluster), after Ref. 3. Size distributions of SFT observed in copper induced by (b) neutron irradiation at 300 K (Ref. 20) and by (c) tensile fracture at 300 K. Size distributions of vacancy-type defect clusters in aluminum induced by (e) self-ion irradiation at 127 K and by (f) tensile fracture at 300 K.

scale. The majority of SFT observed in aluminum are not the most stable configurations in the energy calculation, which demonstrates that the static formation energy does not directly correspond to experimental observations. This is because vacancy clusters grow absorbing point defects one after another: the final defect structure does not always fulfill the minimum-energy requirement, although the point-defect reaction is towards lower free energy at each stage.

We must note that the formation energy of such a small cluster cannot be treated correctly with the elastic theory. Atomistic simulations are adopted for small defect clusters,[28,29] but Osetsky *et al.*[29] suggested that the results seriously depend on the reliability of the interatomic potential function. In this discussion, we assume that the final defect configuration is determined when the vacancy cluster grows to the size where the elastic theory becomes a good approximation. In addition, we take into account the following two points from the calculated formation energy for a qualitative interpretation of SFT formation: (1) When the vacancy cluster is small, SFT have the lowest formation en-

ergy in the three defect configurations. In the middle and larger defect sizes, faulted and perfect dislocation loops have the lowest energy, respectively. (2) The ranges in the defect size where SFT or faulted dislocation loops have the lowest energy are narrower in aluminum than in copper, because of the high stacking-fault energy in aluminum.

A vacancy cluster nucleates, continues to grow as a SFT with absorbing vacancies, and then reaches the critical size where the faulted dislocation loop has less energy than SFT. A conversion from SFT to the faulted dislocation loop takes place if the potential barrier for the conversion is low enough. Because it is natural to consider that the barrier is lower for smaller defects, the conversion will be easy in aluminum. Then vacancy-type dislocation loops have been frequently observed in aluminum. But if the SFT absorbs a large number of vacancies in a period shorter than the average time required for conversion, the cluster must grow as SFT, which will make the conversion more difficult. If we regard the conversion as a thermal activation process, the time required for conversion becomes longer at lower temperatures. In addition, intense irradiation will increase the absorption rate of vacancies. Therefore, intense irradiation at lower temperature is preferable for SFT formation in aluminum.

The first observation of SFT in aluminum by tensile fracture[4] confirmed the stable formation of SFT in this material. The result, however, did not seem to exclude the possibility of the direct formation of SFT, for example, due to reactions of dislocations under plastic deformation.[30] The present experimental results clearly show that the reactions of vacancies can form SFT in aluminum as well as in the other fcc metals. Simultaneously, the results indicate that the range in defect size where SFT are most stable is present in aluminum and that the extent of the range will be smaller than in the other fcc metals.

V. CONCLUSIONS

After the first observation of SFT in aluminum induced by tensile fracture, we conducted experiments on high-energy particle irradiation of aluminum to reexamine whether or not SFT are formed by irradiation in aluminum. The conclusions obtained from the present study can be summarized as follows.

(1) 2-MV electron irradiation induced SFT of an average size of 2 nm below 203 K. A larger irradiation intensity at a lower temperature induced SFT with a larger number density.

(2) 60-keV Al^+ ion irradiation induced SFT below room temperature. The defect yield was about 10^{-3}, considerably smaller than in the other fcc pure metals.

(3) Fission neutron irradiation below 15 K did not induce SFT at a fluence of 2×10^{21} neutrons m^{-2}. Instead, dislocation loops were observed to form and disappear during observation with 120-kV electrons that do not cause atomic displacements. Submicroscopic defect clusters are suggested to form cascade damage.

(4) Tensile fracture of aluminum thin foil induced SFT up to 400 K, which is close to the temperature where SFT become unstable in isochronal annealing experiments. Tensile fracture induces a very high concentration of vacancies.

(5) A high concentration of vacancies supplied at low temperature is a preferable condition to form SFT in aluminum.

*Present address: Institute for Materials Research, Tohoku University, Katahira 2-1-1, Aoba-ku, Sendai 980-8577, Japan.

†Deceased.

[1] P. B. Hirsch, J. Silcox, R. E. Smallman, and K. H. Westmacott, Philos. Mag. **3**, 897 (1958).

[2] B. L. Eyre, J. Phys. F: Met. Phys. **3**, 422 (1973).

[3] S. J. Zinkle, L. E. Seitzman, and W. G. Wolfer, Philos. Mag. A **55**, 11 (1987).

[4] M. Kiritani, Y. Satoh, Y. Kizuka, K. Arakawa, Y. Ogasawara, S. Arai, and Y. Shimomura, Philos. Mag. Lett. **79**, 797 (1999).

[5] M. Kiritani, K. Yasunaga, Y. Matsukawa, and M. Komatsu, Radiat. Eff. Defects Solids **157**, 3 (2002).

[6] Y. Satoh, H. Taoka, S. Kojima, T. Yoshiie, and M. Kiritani, Philos. Mag. A **70**, 869 (1994).

[7] O. S. Oen (unpublished).

[8] K. Urban (unpublished).

[9] Y. Ogasawara, Y. Satoh, S. Arai, and M. Kiritani, Radiat. Eff. Defects Solids **139**, 287 (1996).

[10] Y. Kizuka, Y. Satoh, S. Arai, and M. Kiritani, Radiat. Eff. Defects Solids **145**, 143 (1998).

[11] M. Horiki, S. Arai, Y. Satoh, and M. Kiritani, J. Nucl. Mater. **255**, 165 (1988).

[12] A. Y. Stathopoulos, C. A. English, B. L. Eyre, and P. B. Hirsch, Philos. Mag. A **44**, 309 (1981).

[13] N. Yoshida and M. Kiritani, J. Phys. Soc. Jpn. **35**, 1418 (1973).

[14] R. W. Balluffi, J. Nucl. Mater. **69&70**, 240 (1978).

[15] M. Kiritani, N. Yoshida, H. Takata, and Y. Maehara, J. Phys. Soc. Jpn. **38**, 1677 (1975).

[16] K. Arakawa, K. Satori, S. Arai, and M. Kiritani, Trans. Mater. Res. Soc. Jpn. **16A**, 365 (1994).

[17] T. Yoshiie and M. Kiritani, Mater. Sci. Forum **15−18**, 889 (1987).

[18] K. Arakawa, S. Arai, H. Orihara, K. Ono, and M. Kiritani, J. Electron Microsc. **51**, S225 Suppl (2002).

[19] Y. Satoh, T. Yoshiie, I. Ishida, and M. Kiritani, Philos. Mag. A **80**, 2567 (2000).

[20] Y. Satoh, I. Ishida, T. Yoshiie, and M. Kiritani, J. Nucl. Mater. **155−157**, 443 (1988).

[21] T. Yoshiie, Y. Satoh, H. Taoka, S. Kojima, and M. Kiritani, J. Nucl. Mater. **155−157**, 1098 (1988).

[22] M. Kiritani, J. Phys. Soc. Jpn. **40**, 1035 (1976).

[23] K. Kitagawa, K. Yamakawa, H. Fukushima, T. Yoshiie, Y. Hayashi, H. Yoshida, Y. Shimomura, and M. Kiritani, J. Nucl. Mater. **133&134**, 395 (1985).

[24] M. Kiritani, M. Hoshino, H. Kato, H. Matsui, and N. Matsunami, J. Nucl. Mater. **191−194**, 1128 (1992).

[25] M. L. Jenkins, M. A. Kirk, and W. J. Phythian, J. Nucl. Mater. **205**, 16 (1993).

[26] Y. Satoh, S. Kojima, T. Yoshiie, and M. Kiritani, J. Nucl. Mater. **179−181**, 901 (1991).

[27] M. Kiritani, T. Yoshiie, S. Kojima, and Y. Satoh, Radiat. Eff. Defects Solids **113**, 75 (1990).

[28] Y. Shimomura and R. Nishiguchi, Radiat. Eff. Defects Solids **141**, 311 (1997).

[29] Y. N. Osetsky, A. Serra, M. Victoria, S. I. Golubov, and V. Priego, Philos. Mag. A **79**, 2259 (1999).

[30] M. H. Loretto, L. M. Clarebrough, and R. L. Segall, Philos. Mag. **11**, 459 (1965).